Deformation Behavior of Ferrite-Austenite Duplex High Nitrogen Steel

Byoungkoo Kim, T. T. T. Trang, and Nack J. Kim[*]

POSTECH, Graduate Institute of Ferrous Technology, Pohang 790-784, Korea

The tensile deformation behavior of ferrite-austenite duplex high nitrogen steel has been investigated by interrupted tensile tests and compared with that of fully austenitic high nitrogen steel. It shows that ferrite is softer than austenite and most of the strain in early and later stages of deformation is accommodated by ferrite, while austenite undergoes a deformation-induced martensitic transformation. Such accommodation of a large amount of strain in ferrite is responsible for rapidly increasing work hardening rate and the resultant higher ultimate tensile strength of duplex high nitrogen steel as compared to those of fully austenitic high nitrogen steel, although duplex steel contains a smaller amount of N than austenitic steel.

Key words: high nitrogen steel, duplex steel, deformation behavior, TRIP, work hardening

1. INTRODUCTION

AISI 300 series stainless steel is one of the most widely used steel products owing to excellent corrosion and oxidation resistance, high strain hardening capacity and good ductility [1]. Moreover it can maintain its excellent properties over a wide temperature range from cryogenic to very high temperatures [2]. However it contains rather large amounts of Ni and Mo, which increase its price making the alloy not cost-effective. Therefore, there have been numerous studies to substitute Ni and Mo with cheaper elements such as Mn and N [3,4]. While both Mn and N can increase the stability of austenite, N is more preferable to Mn since the effect of N on corrosion resistance is more positive than that of Mn [5]. Nevertheless, the utilization of N as an alloying element for austenitic steels has not been widely pursued mainly because of its limited solubility in Fe at atmosphere pressure. For example, the solubility of N in liquid Fe is limited to 450 ppm at 1600 °C and atmosphere pressure and the maximum N content which can be alloyed in ferritic and austenitic steels are limited to 800 ppm and 3000 ppm, respectively [6]. However, the recently developed pressurized vacuum induction melting technique makes it possible to make liquid Fe with N content more than 3000 ppm, which can even further be extended by the addition of other alloying elements.

Austenitic high N steels (HNSs) are very promising because of their excellent combination of high strength and high ductility, and good corrosion resistance, which are very similar to those of commercial stainless steels. In addition, they also

provide non-allergic properties, no magnetism with low price as compared to Ni alloyed stainless steels [7,8], which are ideal for applications in transportation, building, aerospace, ocean sports, nuclear power industries as well as military applications [9]. It has been shown that the yield strength of austenitic HNSs can reach 3 GPa by utilizing strain hardening and in most cases such increase in yield and ultimate tensile strength can be obtained. Therefore, there have been numerous studies on high strain hardening rate of austenitic HNS and it has been suggested that grain boundary hardening, strain aging, transformation-induced plasticity (TRIP), twinning-induced plasticity (TWIP) and dislocation planar slip are all related with strain hardening behavior of austenitic HNSs [5,7,8,10].

Since the relative contributions of the above-mentioned deformation modes would vary depending on the stacking fault energy, it is expected that austenitic HNSs would show different deformation behavior depending on their N contents. It shows that the major deformation mode is TRIP and TWIP at low and high N contents, respectively [4,11]. The mechanism of dislocation gliding has also been shown to change from planar type to wavy type with increasing N content.

When austenite phase is present along with ferrite, i.e., such as in duplex stainless steels (DSSs) consisting of ferrite and austenite, they could exhibit mechanical properties and corrosion resistance superior to their single phase counterparts. Despite the technical importance of duplex HNSs, however, only a few studies have been made on the mechanical properties and deformation behavior of the HNSs consisting of duplex austenite and ferrite phases [12]. The objective of the present research is to investigate the deformation behavior of duplex HNS with comparison to that of austenitic HNS.

*Corresponding author: njkim@postech.ac.kr

Table 1. Chemical compositions of Fe-18Cr-10Mn-xN high nitrogen steels (wt%)

	C	Si	Mn	Ni	Cr	Mo	N	Phase
HNS32	0.02	0.42	9.49	0.29	17.50	0.29	0.32	$\alpha + \gamma$
HNS45	0.02	0.36	10.23	0.38	18.00	0.24	0.45	γ

2. EXPERIMENTAL PROCEDURES

The high N steels with different N contents, 0.32 wt% and 0.45 wt%, were fabricated by the pressurized vacuum-induction melting up to 4 bar nitrogen pressure. The chemical compositions of the steels are shown in Table 1. The ingots were cut in 75 mm thickness square block and hot rolled into 25 mm thickness plate at 1250 °C followed by water quenching. The plates were then normalized at 1050 °C for 1 h and water quenched. Longitudinal tensile tests were conducted using specimens with a gage length of 10 mm, a gage width of 2 mm, and a gage thickness of 1 mm at a strain rate of 10^{-3}/s. The microstructure was analyzed by optical microscopy (OM), scanning electron microscopy (SEM), transmission electron microscopy (TEM), and electron back-scatter diffraction (EBSD). The interrupted tensile tests were conducted using five strain steps, 10, 20, 30, 40 and 50%. The volume fractions of constituent phases were measured by EBSD, X-ray diffraction (XRD), and feritscope. For the reliable EBSD anal-

yses, a large area (650 μm × 1800 μm) was scanned to include a large number of grains (900 grains).

3. RESULTS

3.1. Microstructure and tensile properties

Figure 1 shows the optical microstructures of HNS32 and HNS45. The microstructure of HNS32 consists of 5 vol.% ferrite and 95 vol.% austenite. It can be seen that ferrite phase exists as thin bands elongated along the rolling direction. The microstructure of HNS45 is fully austenitic, containing annealing twins within grains. The average grain sizes of HNS32 and HNS45 are 35 μm and 50 μm, respectively.

Tensile properties of these alloys were measured along the rolling direction and their engineering stress-strain curves are shown in Fig. 2(a) along with the curves of their work hardening rate as a function of strain (Fig. 2b). It shows that the duplex HNS32 has lower yield strength (448 MPa) than austenitic HNS45 steel (509 MPa). However, it can also be seen that HNS32 has a much higher ultimate tensile strength (1008 MPa) than HNS45 (890 MPa), although the yield strength of the HNS32 is lower than that of HNS45. HNS32 also shows a sigmoidal stress-strain curve, suggesting the occurrence of deformation-induced martensitic transformation of austenite during tensile deformation. Normalized work hardening rate of HNS32 rapidly increases after a strain of ~12%, also suggesting the occurrence of deformation-induced martensitic transformation of austenite in HNS32.

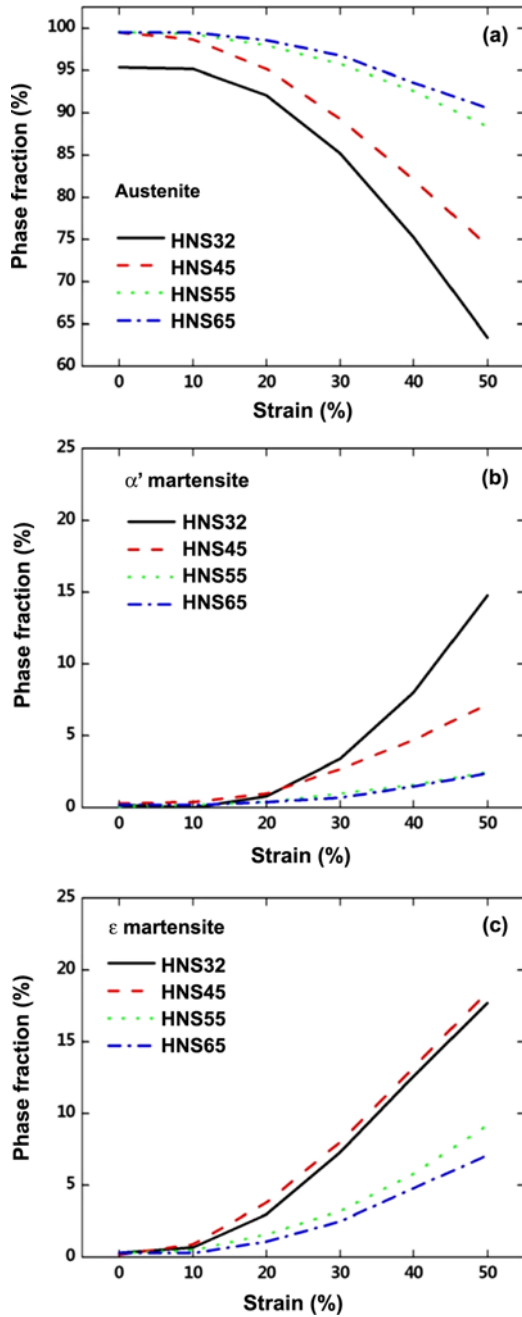### 3.2. Deformation-induced transformation of austenite

The change in the volume fractions of constituent phases during tensile deformation has been analyzed as shown in
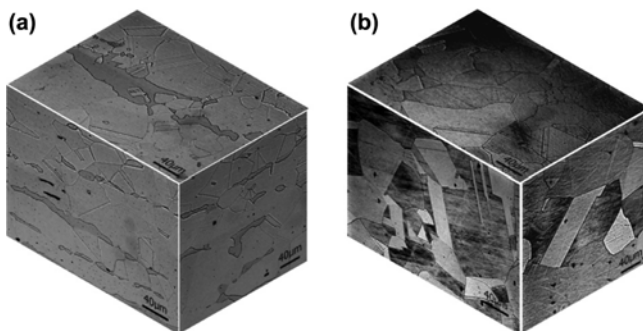
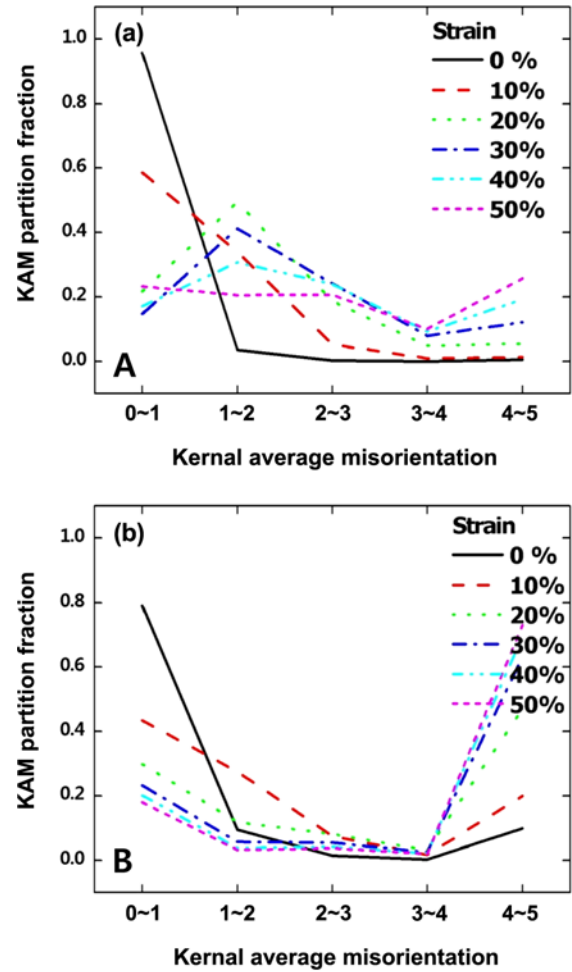**Fig. 1.** Optical microstructure; (a) HNS32 and (b) HNS45.
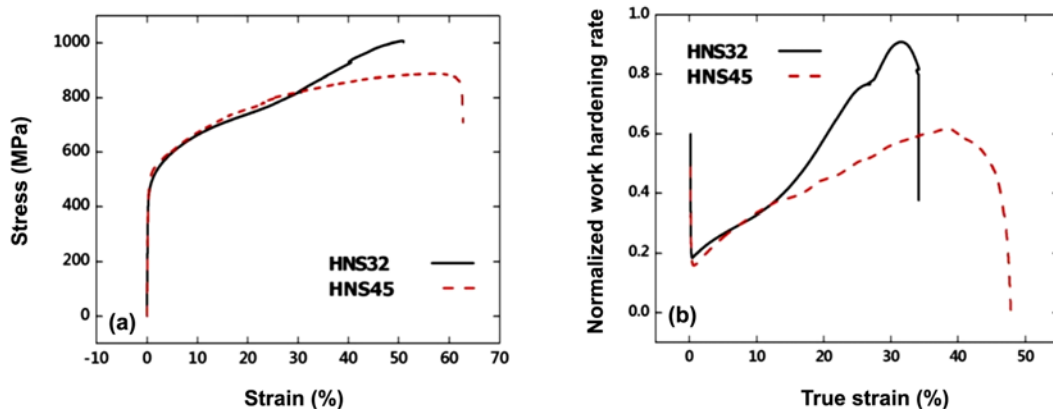
Fig. 2. (a) Engineering stress-strain curves of, HNS32, and HNS45, and (b) normalized work hardening rates as a function of strain.

Fig. 3. The change in the volume fractions of constituent phases during tensile deformation; (a) austenite, (b) α'-martensite, and (c) ε-martensite.

Fig. 4. Fractions of (a) austenite and (b) ferrite as a function of KAMs in HNS32 after deformation.

Fig. 3. It shows that the volume fraction of austenite gradually decreases with increasing strain in duplex HNS32. Such decrease in the volume fraction of austenite with increasing strain in HNS32 is replaced by the increases in the volume fractions of α'-martensite as well as ε-martensite. It further shows that the increase in the volume fraction of α'-martensite is a bit smaller than that of ε-martensite in HNS32 (Figs. 3b and c). The fully austenitic HNS45 shows a similar degree of change in the volume fraction of austenite up to the strain

of 25% to that of duplex HNS32. After the strain of 25%, however, HNS32 shows a larger change in the volume fraction of austenite than HNS45. As is the case of HNS32, most of the deformation-induced transformation of austenite in HNS45 is to ε-martensite rather than to α'-martensite.

One interesting observation made in the present study is that although the degree of deformation-induced transformation of austenite to martensite is quite similar in both HNS32 and HNS45 up to the strain of 25%, HNS32 shows a much higher normalized work hardening rate than HNS45 since the onset of tensile deformation as shown in Fig. 2(b). To understand the origin of such rather unusual behavior of HNS32, detailed EBSD analyses of the tensile deformed specimens were conducted. The specimens were polished prior to tensile testing and the same area was observed before and after tensile deformation up to 30% and the change in kernel averaged misorientations (KAMs) of ferrite and austenite with strain was measured as shown in Fig. 4. Here, the contributions from the newly formed martensite by deformation

can be neglected since the size of the martensite is much smaller (0.1-0.3 μm) than the step size (2 μm). It shows that the fraction of KAMs near high angles (i.e., >3°) are larger in ferrite than in austenite at the same amount of tensile strain. There is a rapid increase in the fraction of KAMs near 4° in ferrite after the tensile strain of 20%. On the other hand, the fraction of KAMs near 4° does not change much in austenite with increasing the amount of tensile strain. This indicates that there is a more partitioning of strain in ferrite than in austenite during tensile deformation, as observed in other duplex steel [13].

4. DISCUSSION

As mentioned previously, the most important observation made in the present study is the much higher work hardening rate of duplex HNS32 than that of fully austenitic HNS45. Since the deformation behavior of austenite varies depending on its SFE, which is also a function of N content, it can be expected that such difference in work hardening rate between two steels might be due to the differences in deformation behavior. It has been recently shown that the deformation-induced transformation of austenite to ε-martensite is more effective for work hardening than the deformation-induced transformation of austenite to α'-martensite [14,15]. However, as shown in Fig. 3(a), the degree of deformation-induced transformation of austenite is much similar in both steels up to the strain of 25%. In addition, both steels show similar amounts of the by-products of such deformation-induced transformation of austenite, i.e., α'-martensite and as ε-martensite at a given strain as shown in Figs. 3(b) and (c). Therefore, the deformation-induced transformation of austenite cannot be responsible for the difference in work hardening rate in HNS32 and HNS45. More importantly, it cannot explain the rapidly increasing work hardening rate of HNS32 as compared to that of HNS45 after the strain of 12%. Figure 5 shows the deformed microstructure of HNS32 and HNS45.

It shows that there is virtually no difference in the deformation modes in austenite between HNS32 and HNS45. The above analyses strongly suggest the important role of ferrite in enhancing the work hardening rate of duplex HNS32 over that of austenitic HNS45.

It is well known that the incorporation of soft phase in hard matrix such as in dual phase (ferrite-martensite) steels can significantly improves the work hardening rate [16]. Such increased work hardening rate in dual phase steels has been ascribed to the presence of mobile dislocations in ferrite and accumulation of dislocations at ferrite/martensite interface. Although the present duplex HNS32 contains different constituent phases, ferrite and austenite, similar phenomena would occur to those of ferrite-martensite dual phase steels if ferrite phase in HNS32 is indeed softer than austenite. Comparing the tensile properties of duplex HNS32 and fully austenitic HNS45, it can easily be deduced that ferrite is softer than austenite, in contrast to previous results on duplex steels containing no or small amounts of N [17-19].

However, the present duplex HNS32 contains a relatively large amount of N, 0.32 wt%, which could be preferentially partitioned in austenite since N is an austenite stabilizer [12]. Such partitioning of N in austenite makes it stronger by solid solution hardening than ferrite. After yielding and work hardening of the softer ferrite phase, sufficient stress is transferred to the harder austenite phase to cause deformation and transformation to martensite [13]. It also results in the build-up of strain along the ferrite/austenite interphase boundaries. As shown in Fig. 6, there is a fairly large amount of dislocations, mostly wavy type, in ferrite grains of HNS32 after the strain of only 5%, while austenite grains are deformed mostly by the planar slip, which is known to have negligible effect on work hardening [20]. It can also be seen that there is a strain accumulation along the ferrite/austenite interphase boundaries. The large strain accommodation capability of ferrite in HNS32 is also evidenced by the results of KAM analyses as shown in Fig. 4. It shows that ferrite grains in HNS32 can
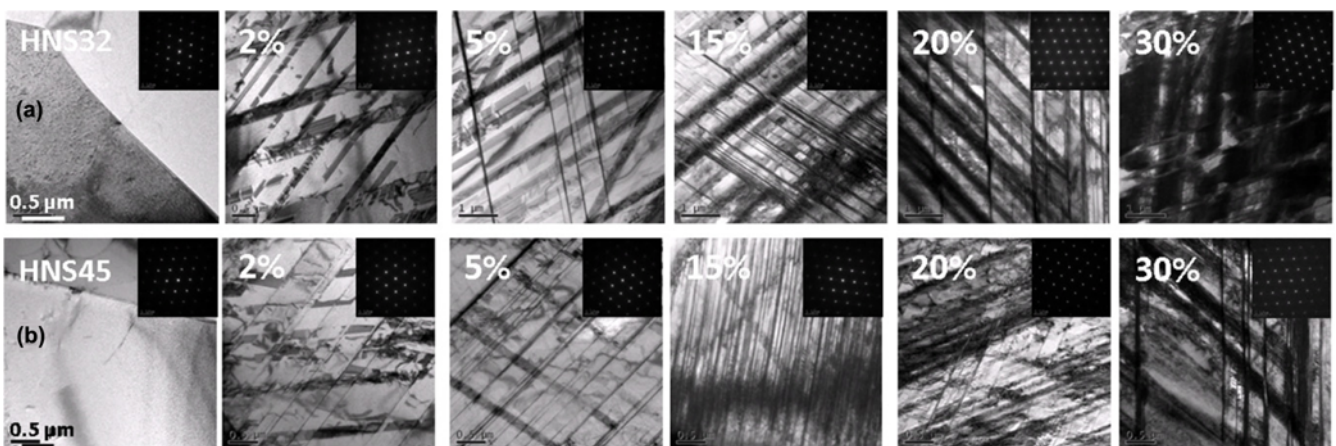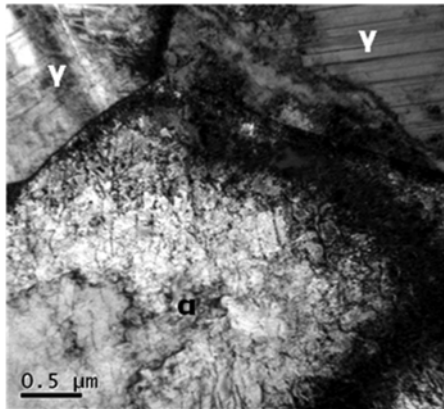

Fig. 5. Deformed microstructure of austenite; (a) HNS32 and (b) HNS45.

Fig. 6. Deformed microstructure of ferrite in HNS32 after tensile strain of 5%.

accommodate a fairly large amount of deformation, while austenite grains do not show the accommodation of strain up to the strain of 50%. Therefore, the presence of ferrite in austenite matrix can significantly increase the work hardening rate of duplex HNS32 by accommodating a large amount of strain in ferrite and effectively transferring the strain to nearby austenite grains in early and intermediate stages of deformation, after which deformation-induced transformation of austenite to martensite plays a dominant role [21]. On the other hand, austenitic HNS45 deforms mostly by planar slip ineffective for work hardening and only relies on deformation-induced transformation of austenite to martensite for work hardening, resulting in lower work hardening rate and ultimate tensile strength than those of duplex HNS32.

5. CONCLUSIONS

A study has been made on the deformation behavior of ferrite-austenite duplex HNS, in comparison with that of a fully austenitic HNS45. It shows that duplex HNS32 shows a higher ultimate tensile strength along with higher work hardening rate than austenitic HNS45, despite the former's lower N content than the latter's. Both steels show similar degree of deformation-induced transformation of austenite to martensite upon deformation, and therefore such deformation-induced transformation of austenite to martensite is not responsible for enhanced work hardening rate of duplex HNS32. On the other hand, the presence of small volume fraction of ferrite in duplex HNS32 is found to be responsible for its rapidly increasing work hardening rate with strain. Ferrite grains in duplex HNS32 can accommodate a large amount of strain and effectively transfer the strain to nearby austenite grains in early and intermediate stages of deformation. On the other hand, austenitic HNS45 deforms mostly by planar slip, which is ineffective for work hardening, resulting in lower work hardening rate and ultimate tensile strength

than those of duplex HNS32.

REFERENCES

1. F. K. Yan, G. Z. Liu, N. R. Tao, and K. Lu, *Acta Mater.* **60**, 1059 (2012).
2. T. S. Byun, N. Hashimoto, and K. Farrell, *Acta Mater.* **52**, 3889 (2004).
3. O. Bouaziz , S. Allain, C. P. Scott, P. Cugy, and D. Barbier, *Current Opinion in Solid State and Materials Science* **15**, 141 (2011).
4. T.-H. Lee, C.-S. Oh, S.-J. Kim, and S. Takaki, *Acta Mater.* **55**, 3649 (2007).
5. T.-H. Lee, C.-S. Oh, and S.-J. Kim, *Scripta Mater.* **58**, 110 (2008).
6. J. W. Simmons, *Mater. Sci. Eng. A* **207**, 159 (1996).
7. V. G. Gavriljuk and H. Berns, *High Nitrogen Steels*, pp.281-284, Springer-Verlag, Berlin (1999).
8. U. Kamachi Mudali and Baldev Raj, *High Nitrogen Steels and Stainless Steels*, p.252, Narosa Publication House, New Delhi (2004).
9. M. O. Speidel, *Met. Sci. and Heat Treatment* **47**, 489 (2005).
10. P. Millner, C. Solenthaler, P. J. Uggowitzer, and M. O. Speidel, *Acta Metall. Mater.* **42**, 2211 (1994).
11. J. Y. Choi, J. H. Ji, S. W. Hwang, and K. T. Park, *Mater. Sci. Eng. A* **534**, 673 (2012).
12. J. Y. Choi, J. H. Ji, S. W. Hwang, and K. T. Park, *Mater. Sci. Eng. A* **535**, 32 (2012).
13. C.-H. Seo, K. H. Kwon, K. Choi, K.-H. Kim, J. H. Kwak, S. Lee, and N. J. Kim, *Scripta Mater.* **66**, 519 (2012).
14. K. H. Kwon, J. S. Jeong, J.-K. Choi, Y. M. Koo, Y. Tomota, and N. J. Kim, *Met. Mater. Int.* **18**, 751 (2012).
15. K. H. Kwon, B.-C. Suh, S.-I. Baik, Y.-W. Kim, J.-K. Choi, and N. J. Kim, *Sci. Technol. Adv. Mater.* **14**, 014204 (2013).
16. N. J. Kim and G. Thomas, *Metall. Trans. A* **12**, 483 (1981).
17. S. Harjo, Y. Tomota, P. Lukáš, D. Neov, M. Vrána, P. Mikula, and M. Ono, *Acta Mater.* **49**, 2471 (2001).
18. N. Jia, R. Lin Peng, D. W. Brown, B. Clausen, and Y. D. Wang, *Metall. Mater. Trans. A* **39**, 3134 (2008).
19. L. Fu, Z. Li, H. Wang, W. Wang, and A. Shan, *Scripta Mater.* **67**, 297 (2012).
20. K. Choi, C.-H. Seo, H. Lee, S. K. Kim, J. H. Kwak, K. G. Chin, K.-T. Park, and N. J. Kim, *Scripta Mater.* **63**, 1028 (2010).
21. J.-Y. Park and Y.-S. Ahn, *Korean J. Met. Mater.* **50**, 793 (2012).